3-D Printed Biocompatible Micro-Bellows Membranes

Khalil Moussi[iD], *Member, IEEE*, and Jurgen Kosel[iD], *Senior Member, IEEE*

Abstract—**Bellows membranes are essential elements in many actuator devices. Currently, the size, shape, and dimensions of bellows membranes are limited by the fabrication process constraints. Miniaturizing the bellows membranes is a prerequisite for the development of integrated systems with novel capabilities as needed, for example, in advanced biomedical devices. Using a two-photon polymerization, 3-D printing technique, we present a high-resolution, high-yield, and customizable manufacturing process to produce Parylene C micro-bellows. An optimization of the crucial design parameters is performed using finite element modeling from which designs with high deflection and low stress were obtained. Different micro-bellows designs are fabricated and characterized. The total volume of the fabricated models ranges from 3 to 0.3 mm^3 and the minimum feature size is 60 μm. The achieved cumulative deflection ranges from 300 to 570 μm.**   **[2017-0307]**

Index Terms—3D printing, miniaturization, micro-bellows membrane, microfabrication, micro device, Parylene C.

I. INTRODUCTION

BELLOWS membranes are one of the most flexible pressure-responsive structures for applications in the low to middle-pressure ranges, and they have been utilized in most pressure transducers, due to their predictable performance [1]–[13]. A bellow membrane is a thin-walled corrugated tube designed to expand or bend easily under longitudinal forces, internal pressure or bending moments [2]. Bellows membranes have been used in a wide range of applications such as thermopneumatic actuators [3], electrostatic actuator [4], microfluidics [5], fuel storage and delivery [6], micro-gripper [7], electrochemical actuators [8], [9], integrated drug delivery actuator [10], [11], artificial tracheal graft [12] and artificial rubber muscle [13]. However, despite the immense progress in various applications, the existing fabrication methods and techniques are still complex, not suitable for mass production, and are especially limited to the macroscale size [3]–[13]. A qualitative and quantitative comparison with the previous fabrication techniques

related to Parylene C bellows is presented in Table I and arranged in a chronological order. The progress in microfabrication methods has spurred the development of complex microsystems with efficientand versatile fabrication processes. A rather emerging manufacturing technique is 3D printing, also known as rapid prototyping. Driven by the growing interest in microdevices and microfabrication, the 3D printing resolution witnessed a remarkable improvement. Especially, the introduction of the two-photon polymerization (TPP) technique allowed 3D printing to overcome the micrometer barrier, achieving a resolution in the nanometer range [14], [15]. TPP was employed in different domains such as microelectromechanical systems [16], biomedical devices [17], [18], micro-photonics and imaging [19], [20], and tissue engineering [21]–[23]. Although this technology offers a very high resolution, it has been used to fabricate structures having a dimension in the millimeter scale and feature size in the micrometer resolution [18]–[23].

In this work, we show the fabrication process to produce micro-bellows membranes with a high degree of design flexibility using TPP 3D printing technology. The process is aimed at providing miniaturization, customized dimensions, and mass production.

Three different micro-bellows designs are studied and optimized using the finite element modeling (FEM) method. 3D printing is used to fabricate master molds, from which Parylene C micro-bellow membranes are derived using a sacrificial mold technique. The fabricated membranes are characterized in terms of their deflection/pressure performance. Finally, the fabrication process is used for implementing two micro-bellows designs that push the limits of miniaturization.
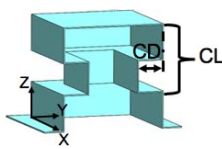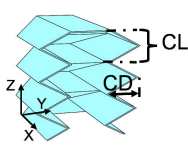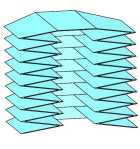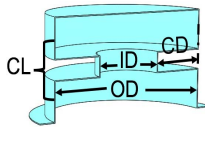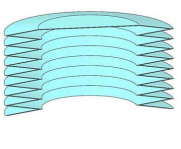
II. MICRO-BELLOWS DESIGNS

Three rectangular and two circular micro-bellows membrane designs were studied based on work done in literature (Table I). The bellows shapes were characterized by the corrugation length (CL) and depth (CD) in addition to the inner diameter (ID) and outer diameter (OD) for the circular models, as shown in Table II. The rectangular membranes are either triangular or rectangular, based on the corrugation cross-section (S1 to S3, in Table II). The rectangular model (S1) had one and a half corrugations. For the triangular cross-section, two models were studied; one composed of three and a half corrugations (S2) and the other one, a miniaturized model, with eight corrugations (S3). In case of the circular membranes, S4 was composed of one and a half corrugations and S5 had 8 triangular corrugations.

TABLE I
SUMMARY OF THE PARYLENE C BELLOWS FABRICATION TECHNIQUES

Ref	Fabrication techniques	Bellows material / thickness	Dimensions	Corrugation cross-section	Corrugation length / depth	Customizable / high yield process
[5]	Wax as a molding / sacrificial material, vapor deposition	Parylene	6 mm diameter	Triangular	NA	not customizable / not a high yield process
[6]	Negative mold by stereolithography, sacrificial wax, vapor deposition	Parylene-PDMS-Parylene / 50-100 μm	10 mm diameter, 12.7-15.6 mm length	Triangular	NA (Minimum feature size of 500 μm)	customizable / not a high yield process
[7]	Micro-stereolithography	Photopolymer (SL5180) / 227-235 μm	2 mm diameter	Rectangular Triangular	500 μm / 500 μm	customizable / not a high yield process
[10]	PDMS mold, sacrificial wax, vapor deposition	Parylene C / 10um	ID 6 mm, OD 9 mm, height 1.6 mm	Rectangular	400 μm / 1.5 mm	not customizable / not a high yield process
[8]	Reusable PDMS, sacrificial wax, vapor deposition	Parylene C / 13.5 μm	ID 5-7 mm, OD 9-10 mm, height 1.2-2.8 mm	Rectangular	400-300 μm / 2.5-1.5 mm	not customizable / not a high yield process
[12]	Sacrificial mold by micro-stereolithography, material injection	poly(ε-caprolactone) / 300 μm to 600 μm	ID 3 mm, 12 mm height	Triangular	800 μm / 1250 μm	customizable / not a high yield process
This work	Reusable 3D printed master mold and PDMS replica, sacrificial wax, vapor deposition	Parylene C / 10 μm	Varies with design, see Table II	Rectangular Triangular	Varies with design, see Table II, (minimum feature size 60 μm)	customizable / a high yield process

TABLE II
DESIGNS AND FEATURES OF THE FABRICATED BELLOWS MEMBRANES

Membrane shape	Rectangular membrane			Circular membrane	
Corrugation cross-section	Rectangular	Triangular		Rectangular	Triangular
Sample reference	S1	S2	S3	S4	S5
3D Design cross-section					
Corrugation number	1.5	3.5	8	1.5	8
Corrugation Length/Depth	500 μm / 300 μm	300 μm / 250 μm	60 μm / 150 μm	300 μm / 700 μm	60 μm / 150 μm
Dimensions X,Y,Z/OD,ID,Z	2-1-1 mm^3	2-1-1 mm^3	1.1-0.6-0.5 mm^3	2-0.8-1 mm^3	1-0.7-0.5 mm^3

III. MODELING AND FEM STUDY

It has been previously shown that analytical models are not suitable to study such membranes, due to the large deflection and the nonlinear nature of Parylene C [8], [24]. However, FEM had shown a good agreement with the experimental data of such complex devices [8], [10]. Thus, FEM was used in this work to optimize the dimensions of the corrugation length and depth for each design, with respect to the largest deflection of the membrane, in addition to an investigation of the stress distribution under different loads.

Different shapes of micro-bellows membranes were designed using Solidworks 2016 (Dassault Systèmes, Vélizy-Villacoublay, France), as shown in Table II. The FEM was implemented for the 3D designs S1, S2 and S4 using the nonlinear static mode and large displacement formulation of Solidworks simulation software. In order to obtain more accurate results, a nonlinear elastic model was implemented. In addition, the data extracted from an experimental stress-strain curve [25] for 10 μm thick Parylene C was defined in the simulation software. The material properties used for the
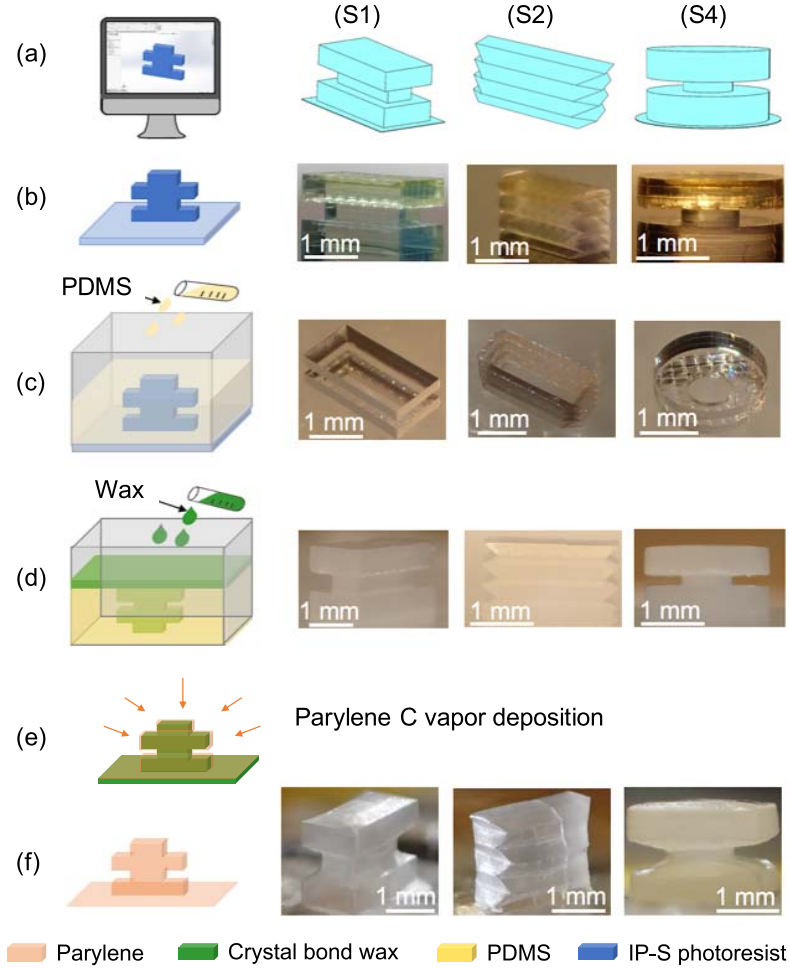
Fig. 1. Fabrication process of Parylene C micro-bellows membranes (samples S1, S2 and S4): (a) 3D designs, (b) 3D printed molds (See supplementary material for the scanning electron microscope (SEM) images of the three different molds), (c) PDMS replicas, (d) sacrificial molds, (e) Parylene C deposition, and (f) 3D Parylene C membranes.

TABLE III

MATERIAL PROPERTIES OF PARYLENE C USED IN FINITE ELEMENT MODELING

Property	Unit	Value
Density	kg/m^3	1289
Young's modulus	MPa	2760
Yield strength	MPa	55.2
Tensile strength	MPa	68.9
Poisson's ratio		0.4

FEM analyses are summarized in Table III. The geometric symmetry of the design was exploited to simplify the simulations, and only a quarter model and a half model were used to simulate the circular and rectangular membranes, respectively.

IV. FABRICATION

The fabrication process of the bellows membranes consists of five steps, as shown in fig. 1, and is described in detail in the following. The 3D printed mold and the PDMS replica are reusable; hence, the fabrication process for the replication of a specific membrane is reduced to only three steps.

A. 3D Printing

After designing the membranes (figure 1a), the Nanoscribe Photonics Professional (GT) system was used to 3D print the re-usable molds shown in figure 1b. A 25x magnification objective lens with a numerical aperture (NA) of 0.8 was selected to achieve dimensions within the millimeter to micrometer scale. The laser had a center wavelength $\lambda = 780$ nm, the power P was 150 mW [26], and the shell scan speed was 50 mm/s. The irradiation intensity at the sample was calculated using the following equation [27]

$$I = \frac{E_p}{\tau_p \pi w^2}, \tag{1}$$

where E_p is the pulse energy, τ_p is the pulse duration ($\tau_p = 100 \ fs$), and w is the beam waist (radius). The pulse energy and the beam waist are expressed as

$$E_p = \frac{P}{f} \tag{2}$$

and

$$w = 0.61 \lambda / NA, \tag{3}$$

respectively. In (2), f is the repetition rate, which is equal to 80 MHz [26]. From (2) and (3), the pulse energy and the beam waist radius are equal to 1.875 nJ and 0.595 μm, respectively. Thus, the irradiation intensity is 1.685 TW/cm^2.

The printed structures were made of IP-S photoresist (Nanoscribe GmbH), a negative-tone photoresist that is characterized by its low shrinkage and smooth surfaces [26]. For sample S1, S2 and S4, both slicing and hatching distances were set to 2 μm. While, for the miniaturized samples S3 and S5, the slicing and hatching distances were set to 1 μm and 0.5 μm, respectively. (see supplementary material, Table S1 summarizes the parameters chosen to convert the STL file into a print job format). The printing configuration was dip-in laser lithography (DILL). The total printing time ranged from 2 hours to 5 hours, depending on the volume of each structure. The 3D molds were developed by immersion in mr-DEV 600 (micro resist technology GmbH, Germany) for 20 minutes followed by a 5 minutes wash in an isopropanol bath and dried with a gentle stream of nitrogen (figure 1b). A post-curing step was performed under 400 nm wavelength UV light with an intensity of 0.2 mW/cm^2 for 30 minutes to strengthen the structures and ensure the total polymerization of the resist (see supplementary material, figure S1-S5 for the scanning electron microscope images of the 3D printed molds).

B. PDMS Replica

The 3D printed structures were used as a master mold to create a negative replica of each design with polydimethylsiloxane (PDMS, Sylgard 184 Silicone Elastomer, Dow Corning Corp., Midland, MI). Using a laser cutter (Universal PLS6.75 10.6 μm CO2), a 25 mm × 25 mm frame of PMMA with 2 mm height was cut and glued to the silicon substrate with the 3D printed mold being located at the center. The frame was filled with PDMS (10:1 base-to-curing agent ratio), desiccated and then cured at 90 °C for 1 hour in the oven. After cooling down to room temperature, the flexible PDMS was pulled off gently from the mold (figure 1c), resulting in a negative replica at the center of the PDMS sample. This process allows reusing the 3D printed structures repeatedly to make multiple PDMS replicas.

C. Sacrificial Mold and Parylene C Deposition

Crystalbond 555 (Ted Pella. Inc.) was used as a sacrificial mold for its low melting temperature (55 °C), non-shrinkage and smooth surface. The molten crystalbond material was poured into the PDMS replicas, and the trapped air bubbles were evacuated manually with the tweezer. Within 30 minutes, the sacrificial molds solidified at room temperature. After removing the PDMS replicas, a sacrificial mold copy of the original 3D printed master mold was obtained (figure 1d). Next, the sacrificial mold was coated with approximately 10 μm of Parylene C (figure 1e) (SCS Labcoter® 2 Parylene Deposition System, Indianapolis, IN), and finally, the membranes were released after immersion in 50 °C deionized water for 30 minutes (figure 1f).

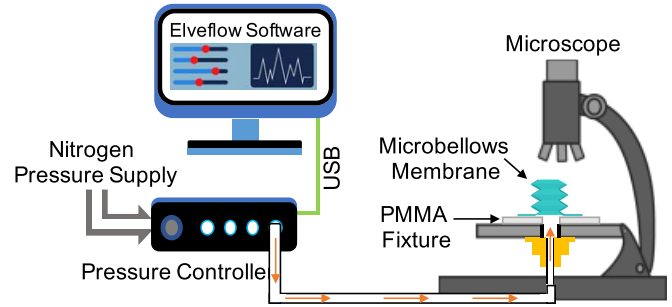Figure 1 shows photos of each fabrication step for the three different membrane types.

Fig. 2.   Micro-bellows membrane load-deflection test setup.

V. Experimental Methods

The 10 μm thick micro bellows membranes were characterized using a custom test setup for pneumatic load deflection (figure 2). Each membrane was glued on top of a custom Poly(methyl methacrylate) (PMMA) test fixture patterned with the laser cutter. The PMMA fixture was connected to a flow controller (Elveflow OB1) that supplied a constant nitrogen pressure (0-200 kPa (0-29 psi)) monitored by the instrument's software. The membranes were expanded by applying pressure from 0 to 120 kPa with an increment of 20 kPa every minute. Using a microscope (PS-888; SEIWA OPTICAL CO. LTD, USA) with a 40× objective lens and 1 μm of vertical resolution, the corresponding deflection of the top surface of the membrane was measured. Initially, the microscope was focused on the membrane, which was in its deflated state, and the fine focus knob was calibrated to zero. At each pressure increment, the focus was readjusted, and the deflection was recorded.

VI. Results and Discussion

A. Finite Element Analysis

The aim of this FEM analysis is to find, for each geometry, (S1, S2 and S4), the optimal corrugation depth and length combinations with respect to the highest deflection, while keeping the stress lower than the yield stress of Parylene C (59 MPa according to [28]), under an applied pressure of 100 kPa. As shown in figure 3 the cumulative deflection for the three different geometries was very sensitive to the corrugation depth, showing a higher deflection for deeper corrugation. However, the variation in corrugation length was only critical for the triangular corrugation model (figure 3b) and slightly affected the other geometries, where the cumulative deflection was inversely proportional to the corrugation length. For the rectangular membrane with rectangular corrugation (figure 3a), the optimal depth and length parameters giving the lowest stress (42 MPa) and maximum deflection (371 μm) were 300 μm and 500 μm, respectively (figure S6 in the supplementary material). For the triangular corrugation design (figure 3b), the optimal depth and length were 250 μm and 300 μm, respectively, leading to a maximum deflection of 530 μm. However, in this model, a higher stress exceeding the yield strength of Parylene C was found for all the sets of corrugation depth and length simulated. This was observed in specific areas of limited size, especially in the folds lines regions (figure S7 in the supplementary material). For the
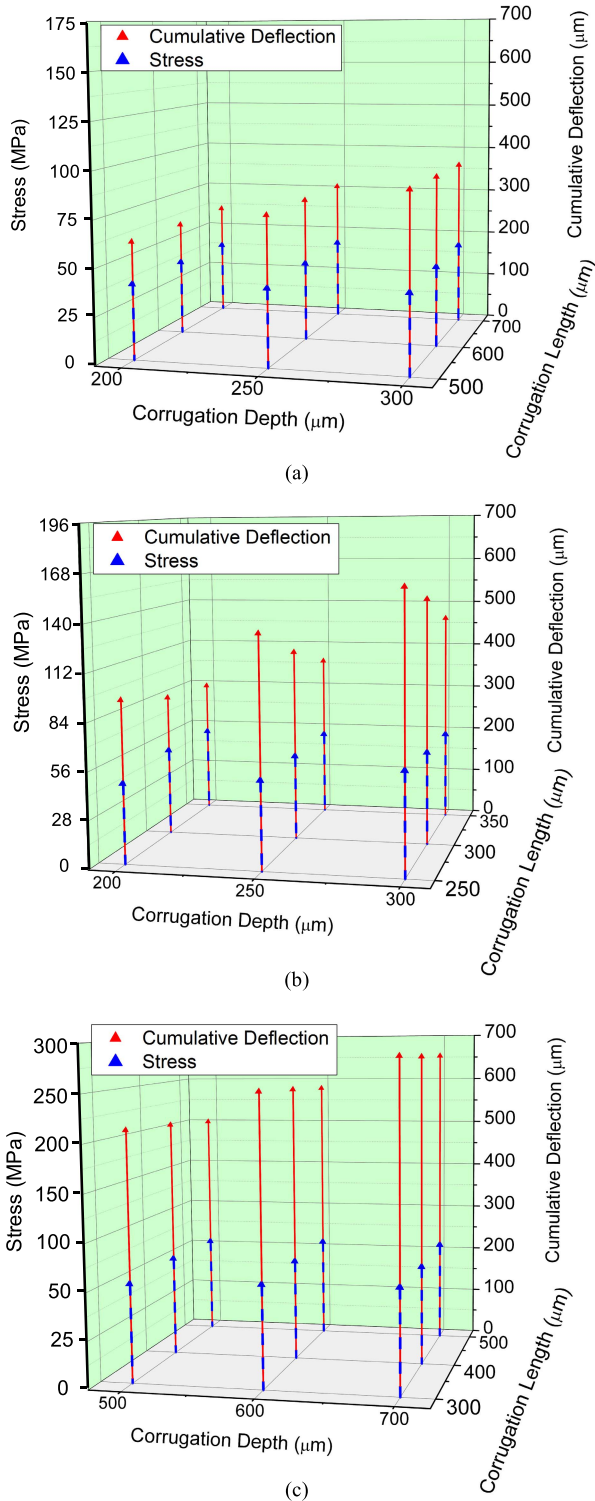
Fig. 3. FEM analyses results of the membranes' cumulative deflection and stress (at 100 kPa) versus corrugation depth and length: (a) rectangular membrane with rectangular corrugation (S1), (b) rectangular membrane with triangular corrugation (S2), and (c) circular membrane with rectangular corrugation (S4).

circular membrane design, the optimal depth and length parameters were 700 μm and 300 μm, respectively, leading to a maximum deflection and stress of 660 μm and 53 MPa, respectively (figure S8 in the supplementary material).
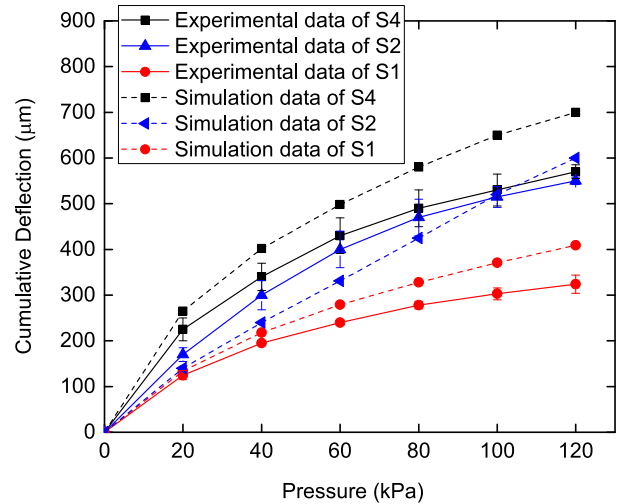

Fig. 4. Load-deflection results showing experimental data and FEM results for the Parylene C micro-bellows membranes S1, S2 and S4 (mean ± SE, n = 3).

B. Experimental Characterization

The Parylene C micro-bellows membranes of the three samples S1, S2, and S4, shown in Table II, were characterized using a custom pneumatic load-deflection test setup (figure 2). Three identical samples from each geometry were tested under the same load conditions, in order to study the reproducibility of the fabrication process and consistency of the characterization tests. As shown in figure 4, for the experimental data, the error for each series of samples was between 2 to 10% of the average deflection value. The circular membrane model achieved the maximum height with a cumulative deflection of 570 μm (57% expansion compared to the initial height of 1 mm) at 120 kPa, which is 25% more than the rectangular membrane with rectangular corrugation. With the triangular corrugation cross-section, which offers a smart folded membrane that can be bent and expanded more than the rectangular corrugation model, similar results as with the circular one were obtained. The rectangular membrane with a triangular corrugation reached a cumulative deflection of 550 μm (55% of expansion compared to the initial height) compared to 320 μm for the rectangular corrugation membrane at an applied pressure of 120 kPa. The FEM results (simulation data in figure 4) were slightly higher than the experimental results, possibly due to an underestimation of Young's modulus, but showed a good trend matching. They showed a larger deviation from the experimental results for the rectangular membrane with a triangular corrugation, which might be, due to the higher number of convolutions (3.5 convolutions) that raise the degree of nonlinearity. The bellows membrane models showed a plastic deformation for pressures exceeding 120 kPa and could withstand up to 200 kPa (the maximum pressure provided by the flow controller used in the load-deflection setup) without bursting. The Parylene C micro-bellows membranes of the miniaturized samples S3 and S5 were characterized using the load deflection setup shown in figure 2. For both samples, the membranes' heights were compressed down to 300 μm. The maximum cumulative deflection reached for S3 and S5 was 600 μm under a maximum pressure of 195 kPa, as shown
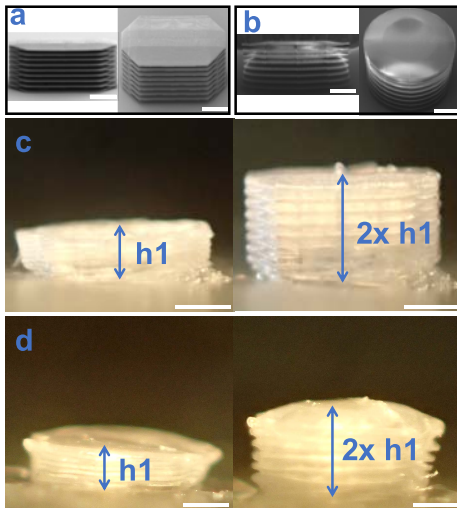
Fig. 5. Load-deflection results of the miniaturized samples S3 and S5. (a)-(b) SEM images of the 3D printed master mold for S3 and S5, (c)-(d) deflection results of S3 and S5 (from an initial height h1 = 300 μm to a maximum deflection of 600 μm). The scale bars are 300 μm.

in figure 5. Compared to the results presented in Table I, the dimensions achieved in S3 and S5 are five times smaller than the minimum feature size reported in [8] and about eight times smaller than the other listed references, while maintaining 100 % cumulative deflection (an initial height of 300 μm and a deflection of 300 μm). In comparison to the Parylene C bellows membrane described by Li *et al.* [10], the external diameter of the circular microbellows model S4 is four and a half times smaller, the initial height is 38% shorter, and the cumulative deflections are 53% and 57% at 100 kPa and 120 kPa, respectively, compared to 111% at 3.5 kPa reported by Li *et al.* [10]. Note that, as the membrane's surface area is reduced the applied pressure becomes higher; however, the load forces are in the same order of magnitude.

VII. Conclusion

We demonstrated the development of universally applicable micro-bellows including the design, FEM parameter optimization, bellows deflection modeling, fabrication process using high-resolution 3D printing and mechanical characterization. Five different designs were studied in detail, out of which three designs were analyzed and compared to the FEM study. The other two models were fabricated in order to study the miniaturization potential of the process. The FEM analysis showed the effect of varying the corrugation depth and length on the membranes' deflection and stress. It turned out that the cumulative deflection is directly proportional to the corrugation depth and inversely proportional to the corrugation length. The mechanical characterization confirmed the FEM results of the micro-bellows deflection, where the maximum total height achieved was 1.57 mm, starting from an initial height of 1 mm (cumulative deflection of 570 μm). We demonstrated the capability of the developed fabrication technique to produce samples with a volume ranging from 3 mm^3 to 0.3 mm^3. Furthermore, a high resolution was achieved, reaching a minimum feature size of 60 μm. By utilizing TPP 3D printing

in the fabrication process, any complex 3D CAD design of micro-bellows can be converted into a final product, allowing customized structures for various applications without altering the fabrication process. Thereby, the 3D printing step, which is rather expensive and time-consuming, is utilized to create a re-usable master mold, making the process cost-effective and suitable for mass production. Moreover, the maximum dimension of the micro-bellows can be scaled down to the sub-millimeter scale, and the minimum feature size can reach up to ($\sim$10 μm). It is also noteworthy that the materials used for the sacrificial mold and final bellows are biocompatible.

References

[1] D. Giovanni, *Flat and Corrugated Diaphragm Design Handbook.* New York, NY, USA: Marcel Dekker, 1982.

[2] J. F. Wilson, "Mechanics of bellows: A critical survey," *Int J. Mech. Sci.*, vol. 26, nos. 11–12, pp. 593–605, 1984.

[3] X. Yang, Y. C. Tai, and C. M. Ho, "Micro bellow actuators," presented at the Transducers Int. Conf. Solid-State Sens. Actuators, Dig. Tech. Papers, vol. 1, 2. New York, NY, USA, 1997. [Online]. Available: http://WOS:A1997BJ35B00007

[4] K. Minami, H. Morishita, and M. Esashi, "A bellows-shape electrostatic microactuator," *Sens. Actuators A, Phys.*, vol. 72, no. 3, pp. 269–276, 1999.

[5] G.-H. Feng and E. S. Kim, "Universal concept for fabricating micron to millimeter sized 3-D parylene structures on rigid and flexible substrates," presented at the IEEE 16th Annu. Int. Conf. MEMS, Kyoto, Japan, 2003.

[6] R. Luharuka, C.-F. Wu, and P. J. Hesketh, "Design, fabrication, and testing of a near constant pressure fuel delivery system for miniature fuel cells," *Sens. Actuators A, Phys.*, vol. 112, no. 2, pp. 187–195, 2004.

[7] H.-W. Kang, I. H. Lee, and D.-W. Cho, "Development of a micro-bellows actuator using micro-stereolithography technology," *Microelectronic Eng.*, vol. 83, no. 4, pp. 1201–1204, 2006.

[8] H. Gensler and E. Meng, "Rapid fabrication and characterization of MEMS Parylene C bellows for large deflection applications," *J. Micromech. Microeng.*, vol. 22, no. 11, p. 115031, 2012.

[9] R. Sheybani, H. Gensler, and E. Meng, "A MEMS electrochemical bellows actuator for fluid metering applications," *Biomed Microdevices*, vol. 15, no. 1, pp. 37–48, Feb. 2013.

[10] P.-Y. Li, R. Sheybani, C. A. Gutierrez, J. T. W. Kuo, and E. Meng, "A parylene bellows electrochemical actuator," *J. Microelectromech. Syst.*, vol. 19, no. 1, pp. 215–228, Feb. 2010.

[11] A. M. Cobo, H. M. Tu, R. Sheybani, and E. Meng, "Characterization of a wireless implantable infusion micropump for small animal research under simulated *in vivo* conditions," in *Proc. BioCAS*, Oct. 2014, pp. 348–351.

[12] J. H. Park, J. W. Jung, H.-W. Kang, Y. H. Joo, J.-S. Lee, and D.-W. Cho, "Development of a 3D bellows tracheal graft: Mechanical behavior analysis, fabrication and an *in vivo* feasibility study," *Biofabrication*, vol. 4, no. 3, p. 035004, 2012.

[13] T. Yanagida, K. Adachi, M. Yokojima, and T. Nakamura, "Development of a peristaltic crawling robot attached to a large intestine endoscope using bellows—Type artificial rubber muscles," in *Proc. IEEE/RSJ Int. Conf. Intell. Robots Syst. (IROS)*, Oct. 2012, pp. 2935–2940.

[14] S. Kawata, H.-B. Sun, T. Tanaka, and K. Takada, "Finer features for functional microdevices," *Nature*, vol. 412, no. 6848, p. 697, 2001.

[15] A. Ostendorf and B. N. Chichkov, "Two-photon polymerization: A new approach to micromachining," *Photon. Spectra*, vol. 40, no. 10, p. 72, 2006.

[16] T. Y. Huang *et al.*, "3D printed microtransporters: Compound micromachines for spatiotemporally controlled delivery of therapeutic agents," *Adv. Mater.*, vol. 27, no. 42, pp. 6644–6650, 2015.

[17] M. Kavaldzhiev, J. E. Perez, Y. Ivanov, A. Bertoncini, C. Liberale, and J. Kosel, "Biocompatible 3D printed magnetic micro needles," *Biomed. Phys., Eng. Exp.*, vol. 3, no. 2, p. 025005, 2017.

[18] Z. F. Rad *et al.*, "High-fidelity replication of thermoplastic microneedles with open microfluidic channels," *Microsyst., Nanoeng.*, vol. 3, p. 17034, Oct. 2017.

[19] T. Gissibl, S. Thiele, A. Herkommer, and H. Giessen, "Two-photon direct laser writing of ultracompact multi-lens objectives," *Nature Photon.*, vol. 10, no. 8, p. 554, 2016.

[20] G. Nelson *et al.*, "Three-dimensional-printed gas dynamic virtual nozzles for X-ray laser sample delivery," *Opt. Exp.*, vol. 24, no. 11, pp. 11515–11530, 2016.

[21] P. Danilevicius *et al.*, "Micro-structured polymer scaffolds fabricated by direct laser writing for tissue engineering," *J. Biomed. Opt.*, vol. 17, no. 8, p. 081405, 2012.

[22] K. S. Worthington *et al.*, "Two-photon polymerization for production of human iPSC-derived retinal cell grafts," *Acta Biomaterialia*, vol. 55, pp. 385–395, Jun. 2017.

[23] A. I. Son *et al.*, "An implantable micro-caged device for direct local delivery of agents," *Sci. Rep.*, vol. 7, no. 1, p. 17624, 2017.

[24] A. C. Ugural, *Stresses in Beams, Plates, and Shells*. Boca Raton, FL, USA: CRC Press, 2009.

[25] B. Lu, "Parylene as a new membrane material for biomems applications," Ph.D. dissertation, Dept. Elect. Eng., California Inst. Technol., Pasadena, CA, USA, 2012.

[26] (Dec. 12, 2017). *Nanoscribe Photonics Professional GT*. [Online]. Available: https://www.nanoscribe.de/en/products/photonic-professional-gt/

[27] M. Malinauskas, P. Danilevičius, and S. Juodkazis, "Three-dimensional micro-/nano-structuring via direct write polymerization with picosecond laser pulses," *Opt. Exp.*, vol. 19, no. 6, pp. 5602–5610, 2011.

[28] C. Y. Shih, T. A. Harder, and Y. C. Tai, "Yield strength of thin-film parylene-C," *Microsyst. Technol.*, vol. 10, no. 5, pp. 407–411, 2004.

Khalil Moussi (M'18) received the B.S. degree in electromechanical engineering and the M.S. degree in robotics from the National Engineering School of Sfax, Tunisia, in 2013 and 2014, respectively. He is currently pursuing the Ph.D. degree in electrical engineering with the King Abdullah University of Science and Technology. His research is focused on the design and fabrication of implantable MEMS devices for drug delivery.

Jurgen Kosel (SM'14) received the Dipl.Ing. (M.Sc.) and Ph.D. degrees in electrical engineering from the Vienna University of Technology, Austria, in 2002 and 2006, respectively. From 2006 to 2007, he was a Project Manager with Magna Powertrain, Austria, in the automotive industry. He was a Post-Doctoral Fellow with the Biomedical Engineering Research Group, Stellenbosch University, South Africa, from 2007 to 2009. He is currently an Associate Professor of electrical engineering with the Computer, Electrical and Mathematical Sciences and Engineering Division, King Abdullah University of Science and Technology, where he is also a Principal Investigator of the Sensing, Magnetism, and Microsystems Research Group.